GMR
The Original

GC-MS-GUIDED DEVELOPMENT AND PRECLINICAL EVALUATION OF A *GLYCINE MAX*-DERIVED PHYTOCOMPOUND-LOADED ZIRCONIA NANOCONSTRUCT IN LETROZOLE-INDUCED POLYCYSTIC OVARY SYNDROME

Ayesha Zubair[1]*, Asma Ahmad[2], Abida Parveen[3], Amir Jalal[4], Sarwat Jahan[5], Asma Hussain[6]

[1,2]Institute of Molecular Biology and Biotechnology, The University of Lahore, Lahore, Pakistan
[3]Senior Registrar, Department of Gynaecology & Obstetrics Unit-3, Allied Hospital-II, Faisalabad Medical University, Faisalabad Pakistan
[4]Assistant Professor, Department of Biochemistry, Sahara Medical College, Narowal, Pakistan
[5]Professor, Department of Pharmacology, Aziz Fatima Medical and Dental College, Faisalabad, Pakistan
[6]Assistant Professor, Department of Physiology, Independent Medical College, Faisalabad, Pakistan
***Corresponding author:** Ayesha Zubair. Email: drayeshazubair@gmail.com

ABSTRACT
Polycystic ovary syndrome (PCOS) is a heterogeneous endocrine-metabolic disorder for which phytochemical and nanocarrier-based strategies are being explored as adjuncts to conventional therapy. This study integrated gas chromatography-mass spectrometry (GC-MS) profiling of polarity-based *Glycine max* (L.) Merr. seed extracts, physicochemical characterization of a carbonic acid, 2-dimethylaminoethyl isobutyl ester-loaded zirconia nanoconstruct (CADIE-ZrO_2), and comparative preclinical testing in letrozole-induced PCOS. GC-MS generated 325 library-matched phytochemical assignments, of which 30 compounds were retained in the finalized research dataset. CADIE-ZrO_2 showed an absorption maximum near 388 nm, FTIR bands compatible with an organic surface-associated layer and the zirconia core, preserved crystalline reflections at approximately 24.8°, 30.2°, 35.1°, 40.3°, 45.2°, 50.4° and 60.2° 2θ, irregular-to-sub-hexagonal morphology with mild agglomeration, a dominant hydrodynamic population near 86 nm, and a mean zeta potential of approximately -31.4 mV. Adult female Wistar rats were allocated to vehicle, letrozole-PCOS, positive-control, four seed-extract, free-CADIE, ZrO_2 and CADIE-ZrO_2 groups. The PCOS group showed persistent diestrus, increased LH and testosterone, and reduced FSH, progesterone and estradiol. CADIE-ZrO_2 reduced LH (1.2 ± 0.4 vs 5.87 ± 0.31 mIU/mL) and testosterone (1.2 ± 0.4 vs 6.15 ± 1.2 ng/dL), while increasing FSH (6.03 ± 0.32 vs 0.03 ± 0.01 mIU/mL) and progesterone (9.72 ± 2.3 vs 4.1 ± 0.6 pg/dL). Ovarian histology showed a marked reduction in cystic pathology with restoration of corpus luteum-containing architecture in the loaded-nanoconstruct group, while uterine, pancreatic, renal and hepatic microarchitecture was largely preserved. Hepatorenal biochemical responses were mixed: urea and creatinine moved toward vehicle values, whereas AST remained elevated. Collectively, the findings support CADIE-ZrO_2 as an exploratory preclinical formulation with selective endocrine and histological benefit, release, pharmacokinetic, biodistribution and longer-term safety studies before translation.

KEYWORDS: polycystic ovary syndrome; *Glycine max*; GC-MS; phytocompound; CADIE; zirconia nanoparticles; nanoconstruct; letrozole; endocrine profile.

1. INTRODUCTION

Polycystic ovary syndrome (PCOS) is a lifelong reproductive-endocrine disorder characterized by combinations of ovulatory dysfunction, hyperandrogenism and polycystic ovarian morphology, with frequent metabolic and psychological comorbidity [1,2]. Contemporary PCOS research therefore increasingly combines endocrine endpoints with ovarian structure, metabolic indices and safety-related measurements.

Oxidative stress, inflammatory signaling, altered gonadotropin dynamics, androgen excess and insulin resistance interact in PCOS pathophysiology [3]. Conventional pharmacological therapy remains clinically important, but treatment is usually symptom-directed and may be limited by tolerability, contraindications or recurrence after discontinuation [1,14]. These considerations have encouraged investigation of plant-derived bioactive compounds and formulation approaches that may influence more than one disease-relevant pathway.

Soybean, *Glycine max* (L.) Merr., contains chemically diverse lipophilic and polar metabolites. The biological profile of a seed extract depends strongly on extraction conditions, and chromatographic profiling is therefore important before biological interpretation. GC-MS is useful for generating a chemically traceable candidate pool, but spectral-library assignments remain tentative unless confirmed against authentic standards.

Nanocarrier systems are being evaluated in PCOS because they may modify dispersion, stability, release and tissue exposure of bioactive payloads [4,5]. Preclinical studies with nanoparticle-associated natural compounds

have reported changes in gonadotropins, androgen status, redox signaling and ovarian histology [6,7]. However, nanomaterial performance depends on size, surface charge, aggregation state, composition and dose; physicochemical characterization must therefore accompany biological testing [4,5].

Zirconia (ZrO_2) is a chemically stable ceramic oxide with surface chemistry compatible with association of organic molecules. The present study used a zirconia platform to formulate carbonic acid, 2-dimethylaminoethyl isobutyl ester (CADIE), a compound retained from the broader *Glycine max* research program. The study focused on three experimental objectives: (i) GC-MS profiling of polarity-based soybean seed extracts, (ii) physicochemical characterization of the CADIE-ZrO_2 formulation, and (iii) comparative in vivo evaluation of seed extracts, free CADIE, ZrO_2 and CADIE-ZrO_2 in a letrozole-induced PCOS model.

2. MATERIALS AND METHODS

2.1. Study design and setting

This experimental study was undertaken at the Institute of Molecular Biology and Biotechnology (IMBB) from November 2025 to February 2026, The University of Lahore, Lahore, Pakistan, with analytical work involving collaborating facilities in Lahore. The study comprised GC-MS profiling, characterization of the loaded zirconia formulation and comparative evaluation in a letrozole-induced PCOS animal model.

2.2. Plant material and polarity-based extraction

Seeds of *Glycine max* (L.) Merr. were obtained from Nawabshah, Sindh, Pakistan. Botanical authentication was performed at the Department of Botany, Government College University, Lahore, and the material was assigned voucher number GC.Herb.Bot.3782. Seeds were ground under hygienic conditions. The extraction sequence used ethyl acetate, n-hexane, chloroform and ethanol, with overnight shaking followed by centrifugation at 4000 rpm for 15 min at each step. Supernatants were retained for downstream analytical work, and extracts were freeze-dried and stored under low-temperature conditions until analysis.

2.3. GC-MS profiling and compound selection

GC-MS profiling was performed at Chughtai Lab, Lahore. Helium (99.99%) was used as carrier gas at 1 mL/min. The oven program began at 60 °C and increased at 10 °C/min to 310 °C; injector temperature was maintained at 250 °C. Mass spectra were compared with NIST20.L and SWGDRUG 3.9.L libraries. Relative percentage abundance was estimated from total-ion-chromatogram peak area. The finalized research dataset retained 30 library-matched compounds from the broader chromatographic output.

2.4. CADIE-ZrO_2 formulation and physicochemical characterization

Zirconia nanoparticles were produced from a zirconium precursor using an aqueous green-synthesis workflow involving precursor preparation, plant-derived reducing/stabilizing material, alkaline hydrolysis/precipitation, centrifugation, washing, drying and calcination where required. CADIE was subsequently associated with the zirconia platform to obtain the surface-loaded formulation used for physicochemical characterization and animal testing.

The loaded formulation was evaluated by UV-visible spectroscopy, Fourier-transform infrared spectroscopy (FTIR), X-ray diffraction (XRD), scanning electron microscopy (SEM), dynamic light scattering (DLS) and zeta-potential analysis. These techniques were interpreted as complementary evidence for optical behavior, surface-associated functional groups, retention of zirconia crystallinity, morphology, hydrodynamic size and colloidal surface charge.

2.5. Animal model, ethical approval and treatment groups

Animal work was performed after approval by the institutional ethics process (UOL/IREB/26/22/07/0010). Adult healthy non-pregnant female albino Wistar rats weighing approximately 150-200 g were acclimatized for at least one week and maintained under controlled environmental conditions with standard diet and water ad libitum. Animals were divided into ten groups with three replicates per group (n=3). PCOS induction used letrozole for 21 days according to the approved study protocol.

Table 1. Experimental groups used for the preclinical PCOS evaluation.

Group	Designation	Treatment
I	Vehicle	DMSO only
II	PCOS negative control	Letrozole, 1.0 mg/mL/kg body weight for 21 days
III	Positive control	PCOS induction + cyproterone acetate 1 mg/kg body weight for 21 days
IV	Experimental	PCOS induction + n-hexane *Glycine max* seed extract, 10 mg/kg
V	Experimental	PCOS induction + ethyl acetate *Glycine max* seed extract, 10 mg/kg
VI	Experimental	PCOS induction + methanolic *Glycine max* seed extract, 10 mg/kg
VII	Experimental	PCOS induction + distilled-water *Glycine max* seed extract, 10 mg/kg
VIII	Experimental	PCOS induction + CADIE, 1.0 mg/kg intraperitoneally

Group	Designation	Treatment
IX	Experimental	PCOS induction + ZrO_2 nanoparticles, 1.0 mg/kg intraperitoneally
X	Experimental	PCOS induction + CADIE-ZrO_2 nanoparticles, 1.0 mg/kg intraperitoneally

2.6. Estrous-cycle monitoring and sample collection

Vaginal smears were collected using 0.9% saline and examined microscopically after staining to identify proestrus, estrus, metestrus and diestrus based on nucleated epithelial cells, cornified cells and leukocytes. Persistent diestrus was used as a pheSypic indicator of letrozole-induced cycle disruption. At study completion, blood was collected under anesthesia according to the approved protocol, serum was separated, and tissues were harvested for morphological and histopathological assessment.

2.7. Hormonal and biochemical measurements

Serum LH, FSH, testosterone, estradiol, progesterone and insulin were evaluated using the immunoassay procedures specified in the study protocol. Biochemical measurements included glucose, ALT, AST, bilirubin, urea, creatinine and uric acid using spectrophotometric or automated chemistry methods. HOMA-IR was calculated as glucose (mmol/L) × insulin (μU/mL) / 22.5.

2.8. Histopathology

Ovary, uterus, liver, kidney and pancreas were collected after euthanasia, washed in normal saline, fixed in 10% neutral buffered formalin, processed through graded alcohol and xylene, embedded in paraffin, sectioned and stained with hematoxylin and eosin. Slides were evaluated microscopically by a histopathologist or trained observer, with blinding to group allocation where possible.

2.9. Statistical analysis

Quantitative data were reported as mean ± standard deviation. GraphPad Prism 8.5 was used for statistical analysis. Multiple-group comparisons were evaluated using two-way analysis of variance (ANOVA), with non-parametric alternatives when assumptions of normality or equal variance were met. A p value <0.05 was considered statistically significant.

3. RESULTS

3.1. GC-MS profile of *Glycine max* seed extracts

GC-MS profiling of the polarity-based *Glycine max* seed extracts generated 325 library-matched phytochemical assignments. Thirty compounds were retained in the finalized research dataset. The largest relative peak areas among these retained entries were observed for undecanoic acid, ethyl ester (25.43%), ethyl oleate (13.07%), 2-propenoic acid, 3-[(phenylmethyl)thio]-, (E)- (9.92%), glycidyl palmitate (4.46%), isopropyl linoleate (4.14%), cis-13,16-docasadienoic acid (3.87%) and campesterol (2.82%). NIST20 match-quality values across the retained dataset ranged from 22 to 99, indicating that confidence in library assignment was uniform. Accordingly, lower-quality matches were interpreted cautiously.

The n-hexane profile included methyl 9-cis,11-trans-octadecadienoate (quality 99; relative area 2.04%) and glycidyl palmitate (quality 95; relative area 4.46%). The ethanolic extract contributed the highest-area retained peaks, including undecanoic acid, ethyl ester (25.43%) and ethyl oleate (13.07%). The chloroform fraction included a 9.92% peak assigned to 2-propenoic acid, 3-[(phenylmethyl)thio]-, (E)-, but the low library-match quality in this fraction warrants tentative interpretation. In the ethyl acetate extract, isopropyl linoleate (4.14%), cis-13,16-docasadienoic acid (3.87%) and campesterol (2.82%) were among the most abundant retained entries.

Table 2. Highest relative peak areas among the 30 retained GC-MS library matches.

Tentative compound assignment	Relative area (%)	Extract	Interpretive note
Undecanoic acid, ethyl ester	25.43	Ethanolic extract	High-abundance retained peak
Ethyl oleate	13.07	Ethanolic extract	High-abundance retained peak
2-Propenoic acid, 3-[(phenylmethyl)thio]-, (E)-	9.92	Chloroform extract	Low library-match quality; interpret tentatively
Glycidyl palmitate	4.46	n-Hexane extract	NIST20 quality 95
Isopropyl linoleate	4.14	Ethyl acetate extract	Among leading ethyl-acetate peaks
cis-13,16-Docasadienoic acid	3.87	Ethyl acetate extract	Among leading ethyl-acetate peaks
Campesterol	2.82	Ethyl acetate extract	NIST20 quality 93

3.2. Physicochemical characterization of CADIE-ZrO_2

The loaded formulation appeared as a creamy-white powder/off-white suspension. UV-visible spectroscopy showed a dominant absorption maximum near 388 nm. FTIR displayed a broad band near 3430 cm^{-1}, a band near 2922 cm^{-1}, a carbonyl-associated feature near 1715 cm^{-1}, bands around 1450 and 1382 cm^{-1}, a signal near 1115 cm^{-1} and a low-frequency zirconia-associated band near 560 cm^{-1}. The combined profile was consistent with an organic surface-associated component while retaining the Zr-O_2 signature.

XRD retained major reflections near 24.8°, 30.2°, 35.1°, 40.3°, 45.2°, 50.4° and 60.2° 2θ, supporting preservation of the crystalline zirconia framework after loading. SEM showed irregular to sub-hexagonal domains with rough boundaries and mild agglomeration. DLS identified a principal hydrodynamic population near 86 nm with a broader minor tail, whereas the mean zeta potential was approximately -31.4 mV, a surface-charge profile compatible with improved electrostatic dispersion stability.

Table 3. Integrated characterization profile of CADIE-ZrO_2.

Parameter	Finding	**Interpretation**
Appearance	Creamy-white powder / off-white suspension	Macroscopic formulation indicator
UV-visible	λmax ≈ 388 nm	Optical response after loading
FTIR	~3430, 2922, 1715, 1450, 1382, 1115 and ~560 cm^{-1}	Surface-associated organic bands with persistent Zr-O_2 feature
XRD	~24.8°, 30.2°, 35.1°, 40.3°, 45.2°, 50.4°, 60.2° 2θ	Crystalline zirconia fingerprint retained
SEM	Irregular to sub-hexagonal domains; rough boundaries; mild agglomeration	Heterogeneous nanoscale morphology
DLS	Dominant population ≈ 86 nm	Hydrodynamic nanoscale population with minor larger tail
Zeta potential	Mean ≈ -31.4 mV	Surface charge compatible with improved colloidal stability

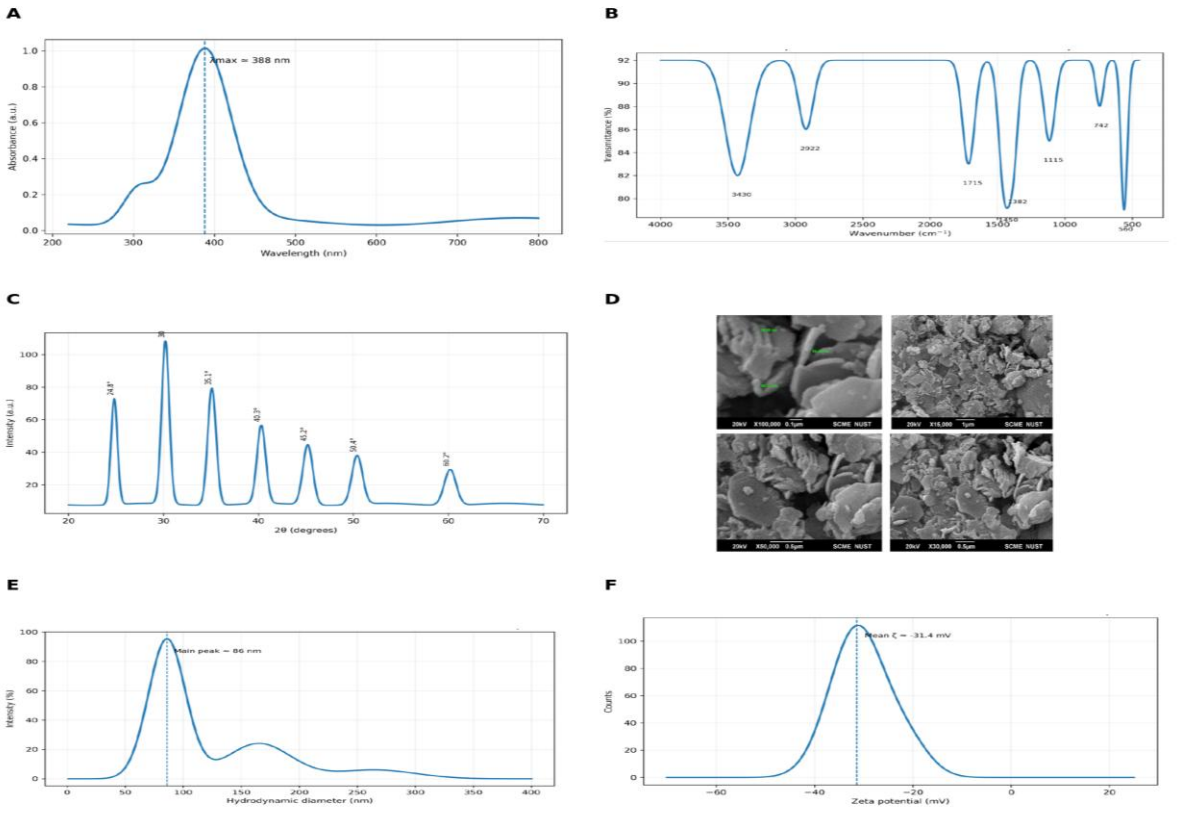

Figure 1. Physicochemical characterization of CADIE-ZrO_2: (A) UV-visible spectrum with λmax near 388 nm; (B) FTIR profile; (C) XRD pattern; (D) SEM micrographs showing irregular morphology and mild agglomeration; (E) DLS particle-size distribution with a dominant population near 86 nm; and (F) zeta-potential distribution with mean surface potential near -31.4 mV.

3.3. Validation of the letrozole-induced PCOS phenotype

Vehicle animals showed normal cyclicity, whereas the letrozole-PCOS group demonstrated an irregular/arrested cycle with persistent diestrus. Representative smears showed the expected changes in nucleated epithelial cells, cornified squamous cells and leukocytes across the estrous phases, with the PCOS condition characterized by persistent leukocyte-dominant diestrus. At the tissue level, the PCOS group showed multiple subcapsular cystic ovarian follicles, loss of the normal corpus-luteum-containing pattern and associated ovarian architectural disturbance.

3.4. Reproductive endocrine response

Letrozole induction increased LH from 1.8 ± 0.21 to 5.87 ± 0.31 mIU/mL and testosterone from 2.0 ± 0.29 to 6.15 ± 1.2 ng/dL, while FSH decreased from 3.14 ± 0.98 to 0.03 ± 0.01 mIU/mL. Progesterone decreased from 7.5 ± 0.5 to 4.1 ± 0.6 pg/dL, and estradiol fell from 96.6 ± 16.07 to 28.3 ± 20.12 pg/mL.

The *Glycine max* extract arms showed endpoint-dependent responses. LH was reduced to 0.5 ± 0 mIU/mL in the distilled-water group and to approximately 0.6 ± 0.28 mIU/mL in the n-hexane, ethyl-acetate and methanolic groups. Testosterone declined to 0.7 ± 0.26, 1.3 ± 0.3, 2.1 ± 0.25 and 3.23 ± 0.1 ng/dL in the distilled-water, methanolic, n-hexane and ethyl-acetate groups, respectively. Progesterone was highest in the methanolic (15.5 ± 8.5) and ethyl-acetate (14.463 ± 3.43) groups, while estradiol recovery was most pronounced with ethyl acetate (78 ± 10.5 pg/mL), followed by methanolic (57 ± 7.2 pg/mL) and n-hexane extracts (47 ± 5.5 pg/mL). These patterns indicate that no single extract was uniformly optimal across all endocrine endpoints.

Among the nanoformulation-related groups, CADIE-ZrO_2 reduced LH to 1.2 ± 0.4 mIU/mL and testosterone to 1.2 ± 0.4 ng/dL. FSH increased to 6.03 ± 0.32 mIU/mL and progesterone to 9.72 ± 2.3. Free CADIE produced FSH of 2.45 ± 1.15 mIU/mL, testosterone of 1.8 ± 1.07 ng/dL, progesterone of 9.05 ± 1.27 and estradiol of 48 ± 5.2 pg/mL. ZrO_2 reduced LH and testosterone but did not restore FSH (0.02 ± 0.01 mIU/mL). Importantly, estradiol in the loaded group was 23 ± 6.08 pg/mL, demonstrating that endocrine recovery.

Table 4. Selected endocrine outcomes for vehicle, PCOS, ZrO_2 and CADIE-ZrO_2 groups.

Outcome	Vehicle	PCOS control	ZrO_2	CADIE-ZrO_2
LH (mIU/mL)	1.8 ± 0.21	5.87 ± 0.31	2.0 ± 0.47	1.2 ± 0.4
FSH (mIU/mL)	3.14 ± 0.98	0.03 ± 0.01	0.02 ± 0.01	6.03 ± 0.32
Testosterone (ng/dL)	2.0 ± 0.29	6.15 ± 1.2	2.23 ± 0.05	1.2 ± 0.4
Progesterone (pg/dL)	7.5 ± 0.5	4.1 ± 0.6	6.31 ± 0.5	9.72 ± 2.3
Estradiol (pg/mL)	96.6 ± 16.07	28.3 ± 20.12	38 ± 16.3	23 ± 6.08

3.5. Hepatic and renal biochemical observations

In the loaded CADIE-ZrO_2 group, ALT was 50.0 ± 4.35 IU/L compared with 28.6 ± 7.09 IU/L in vehicle animals; the corresponding ZrO_2 value was markedly higher at 188.3 ± 2.19 IU/L. AST remained elevated in the loaded group (231.3 ± 23.5 IU/L) and in the free-CADIE group (253.3 ± 25.6 IU/L). ALP was 186 ± 16.64 IU/L in CADIE-ZrO_2 and 195 ± 55.4 IU/L in ZrO_2 animals. These results argue against describing the formulation as demonstrating complete biochemical safety.

Renal-associated indices showed a more favorable direction for selected markers. Urea increased from 25.1 ± 1 mg/dL in vehicle animals to 51.3 ± 1.5 mg/dL in the PCOS group and was lower in CADIE-ZrO_2 animals (33.36 ± 3.7 mg/dL). Creatinine increased from 0.31 ± 0.05 to 0.72 ± 0.1 mg/dL with PCOS and was 0.5 ± 0.1 mg/dL after CADIE-ZrO_2. Uric acid was 3.5 ± 0.15 mg/dL in vehicle, 2.7 ± 1.93 mg/dL in PCOS and 3.9 ± 0.4 mg/dL in the loaded group.

Table 5. Selected renal-associated biochemical indices.

Marker	Vehicle	PCOS control	ZrO_2	CADIE-ZrO_2
Urea (mg/dL)	25.1 ± 1	51.3 ± 1.5	37.3 ± 10.1	33.36 ± 3.7
Creatinine (mg/dL)	0.31 ± 0.05	0.72 ± 0.1	0.65 ± 0	0.5 ± 0.1
Uric acid (mg/dL)	3.5 ± 0.15	2.7 ± 1.93	4.8 ± 2.27	3.9 ± 0.4

3.6. Gross morphology and histopathology

The PCOS negative-control ovary exhibited multiple subcapsular cystic follicles, a 'string-of-pearls'-like appearance, granulosa-layer disturbance and absence of newly formed corpora lutea in the gross/histological description. Kidney sections in this group showed mild tubulointerstitial nephritis and intratubular casts, and the liver showed mild peripheral inflammation. The extract-treated groups demonstrated variable recovery; ethyl-acetate and methanolic treatments were described as showing more pronounced ovarian structural improvement, whereas n-hexane and distilled-water groups showed more partial recovery.

Free CADIE produced moderate ovarian and uterine improvement, while ZrO_2 produced a more limited ovarian response and occasional renal congestion. In the histology series, the CADIE-ZrO_2 panel showed ovarian cortex with corpus luteum and follicles without the prominent cystic pattern, proliferative uterine endometrium, pancreatic acini/islets, renal tissue described as normal, and hepatocytes with preserved lobular architecture. Thus, tissue morphology supported a stronger structural response to the loaded formulation than to the untreated PCOS state, although the concurrent liver-enzyme abnormalities require a cautious safety interpretation.

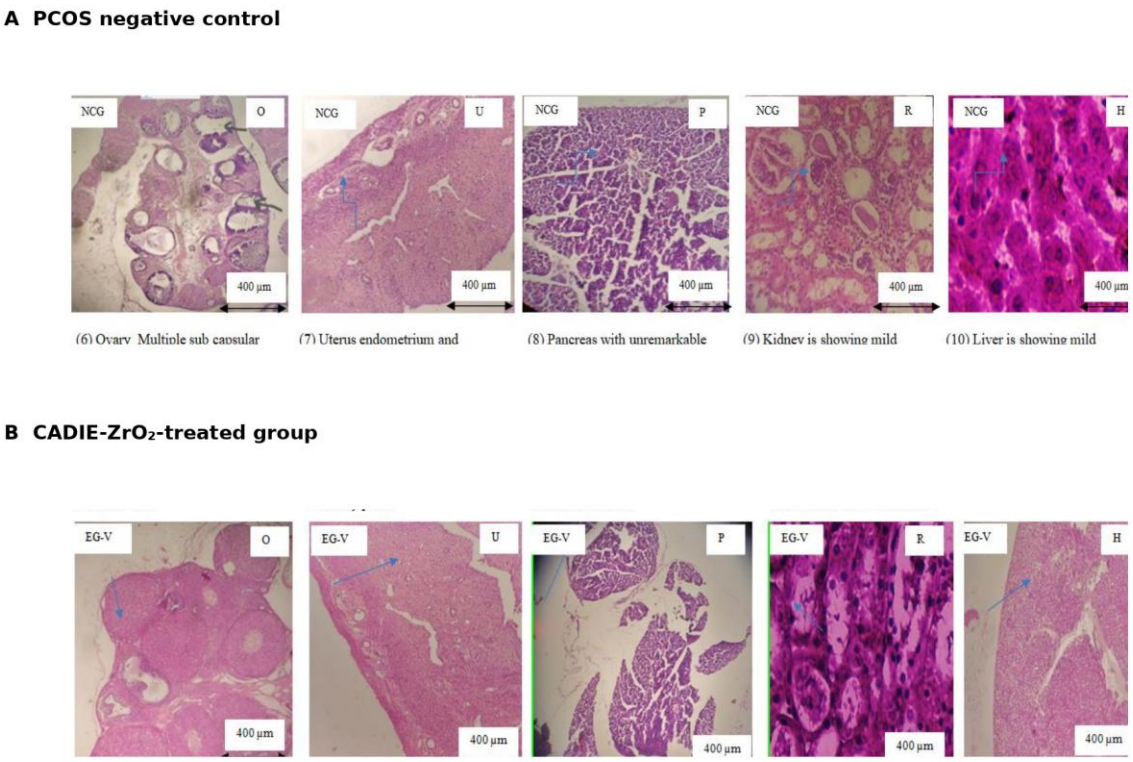

Figure 2. Representative multi-organ histology (original scale bars 400 µm). (A) PCOS negative control: ovary with multiple subcapsular cystic follicles, uterus, pancreas, kidney with reported mild tubulointerstitial changes, and liver with mild peripheral inflammation. (B) CADIE-ZrO_2-treated group: ovarian cortex with corpus luteum/follicles and reduced cystic appearance, proliferative endometrium, pancreatic tissue, renal tissue and hepatic architecture described as preserved.

4. DISCUSSION

This study integrates three experimentally distinct but biologically connected components: chromatographic definition of the soybean-derived candidate pool, physicochemical characterization of a loaded zirconia formulation, and comparative testing in a letrozole-induced PCOS model. Rather, CADIE-ZrO_2 showed a coherent pattern of improvement in several reproductive-hormone and ovarian-structure measures, accompanied with mixed hepatic biochemical findings. This distinction is important for a rigorous preclinical interpretation.

The GC-MS results demonstrate substantial chemical diversity across polarity-based *Glycine max* extracts. The wide range in library-match quality (22-99) also highlights an analytical limitation that is often underemphasized in phytochemical studies. Consequently, this study treats the 30 retained compounds as library-matched candidates rather than definitively identified metabolites. The high relative areas of undecanoic acid ethyl ester and ethyl oleate indicate chromatographic abundance.

The CADIE-ZrO_2 characterization profile provides mutually reinforcing evidence of a surface-modified zirconia system. The 388-nm optical response, coating-associated FTIR bands, retained XRD reflections, SEM morphology, nanoscale DLS population and negative zeta potential together support formulation of a distinct loaded nanoconstruct. The zeta potential near -31.4 mV is particularly relevant to dispersion behavior, whereas the DLS distribution and SEM evidence of mild agglomeration show that particle state depends on measurement environment. Similar nanomedicine literature emphasizes that particle size, surface charge, aggregation and formulation composition can materially change biological behavior [4,5].

The letrozole model generated the expected endocrine direction of PCOS, with elevated LH and testosterone, markedly suppressed FSH and lower progesterone/estradiol, together with persistent diestrus and cystic ovarian pathology. These features are consistent with the utility of letrozole models for studying hyperandrogenic anovulatory PCOS phenotypes. Other preclinical studies have reported improvement in ovarian histology and

endocrine or inflammatory markers after phytochemical or nanoparticle-based interventions [6-9], although differences in formulation, dose and experimental design prevent direct effect-size comparison.

The extract arms showed that solvent-dependent phytochemical composition translated into different endocrine patterns. Distilled-water extract produced the lowest LH and testosterone values, whereas methanolic and ethyl-acetate extracts produced stronger progesterone or estradiol recovery. This divergence supports the concept that botanical preparations act as chemically complex mixtures rather than single-target agents. It also argues against selecting a 'best extract' on the basis of one hormone alone.

The loaded nanoconstruct produced the clearest combined improvement in LH, FSH, testosterone and progesterone among the zirconia-related treatment arms. The contrast with ZrO_2 is informative: zirconia reduced LH and testosterone but did not restore FSH, whereas CADIE-ZrO_2 markedly increased FSH and produced a stronger progesterone response. This pattern is compatible with a payload-associated effect, although the present study establish mechanism, target engagement, tissue-specific delivery or causality at the molecular level.

Estradiol is an important counterpoint. The loaded group did restore estradiol toward the vehicle level and was lower than both free CADIE and ZrO_2 in the dataset. Therefore, the formulation should be described as fully normalizing the hypothalamic-pituitary-ovarian axis. A more defensible interpretation is selective endocrine correction accompanied by ovarian structural recovery. This type of endpoint-specific response is plausible in PCOS, where gonadotropin regulation, steroidogenesis, follicular development and metabolic state are interdependent but not identical processes.

Histological findings provide anatomical support for biological activity. The PCOS group displayed multiple cystic follicles and loss of a normal corpus-luteum pattern, whereas the loaded formulation was associated with corpus luteum-containing ovarian tissue and reduced cystic appearance. The preservation of uterine, pancreatic, renal and hepatic architecture in the loaded-group panels is encouraging. Nevertheless, histology must be interpreted beside biochemistry: AST remained markedly elevated and ALT remained above the vehicle mean. Thus, the current evidence supports preliminary tissue-level tolerability.

5. CONCLUSION

Polarity-based GC-MS profiling of *Glycine max* seeds generated a chemically diverse candidate pool, and the CADIE-loaded zirconia formulation showed a coherent physicochemical profile characterized by retained zirconia crystallinity, nanoscale hydrodynamic size and a negative surface potential. In letrozole-induced PCOS, CADIE-ZrO_2 produced marked improvement in LH, FSH, testosterone, progesterone and ovarian histology relative to the untreated PCOS state, and hepatic enzyme showed improvement.

DECLARAIONS

Ethical Approval

Animal experimentation was conducted under institutional ethical approval UOL/IREB/26/22/07/0010.

Data Availability

The analyzed data reported in this study are contained within the study and the associated institutional research record. Availability of underlying raw files is subject to institutional archiving and author verification.

Conflicts of Interest

The author declares no conflict of interest.

REFERENCES

[1] Hoeger KM, Dokras A, Piltonen T. Update on PCOS: Consequences, challenges, and guiding treatment. The Journal of Clinical Endocrinology & Metabolism. 2021;106(3):e1071-e1083. doi:10.1210/clinem/dgaa839.

[2] Bai H, Ding H, Wang M. Polycystic ovary syndrome (PCOS): Symptoms, causes, and treatment. Clinical and Experimental Obstetrics & Gynecology. 2024;51(5):126. doi:10.31083/j.ceog5105126.

[3] Rudnicka E, Duszewska AM, Kucharski M, Tyczyński P, Smolarczyk R. Oxidative stress in polycystic ovary syndrome. Reproduction. 2022;164(6):F145-F154. doi:10.1530/REP-22-0152.

[4] Butt MA, Tabassum S, Hardy RS, Kiyani MM. Mechanistic insight into nanomedicine for polycystic ovary syndrome. Molecular Biology Reports. 2025;52(1):618. doi:10.1007/s11033-025-10709-7.

[5] Shi M, Li X, Xing L, Li Z, Zhou S, Wang Z, Zou X, She Y, Zhao R, Qin D. Polycystic Ovary Syndrome and the Potential for Nanomaterial-Based Drug Delivery in Therapy of This Disease. Pharmaceutics. 2024;16(12). doi:10.3390/pharmaceutics16121556.

[6] Raja MA, Maldonado M, Chen J, Zhong Y, Gu J. Development and evaluation of curcumin encapsulated self-assembled nanoparticles as potential remedial treatment for PCOS in a female rat model. International Journal of Nanomedicine. 2021;16:6231-6247. doi:10.2147/IJN.S302161.

[7] Rabah HM, Mohamed DA, Mariah RA, Abd El-Khalik SR, Khattab HA, AbuoHashish NA, Abdelsattar AM, Raslan MA, Farghal EE, Eltokhy AK. Novel insights into the synergistic effects of selenium nanoparticles and metformin treatment of letrozole-induced polycystic ovarian syndrome: Targeting PI3K/Akt signalling pathway, redox status and mitochondrial dysfunction in ovarian tissue. Redox Report. 2023;28(1):2160569. doi:10.1080/13510002.2022.2160569.

[8] Rashid S, Khan WY, Hafiz S, Mushtaq Z, Rafiq M, Rasheed S, Ganie SA, Amin S. Ocimum tenuiflorum L. extracts attenuate polycystic ovarian syndrome in letrozole-treated female Wistar rats through modulation of iNOS, COX-2, IL-1β and TNF-α. Journal of Molecular Histology. 2026;57(2):126. doi:10.1007/s10735-026-10774-7.
[9] Bahreiny SS, Khorsandi L, Hoseinynejad K, Ahangarpour A. Chlorogenic acid alleviates letrozole-induced polycystic ovary syndrome in mice by modulating inflammatory mediators and antioxidant signaling pathways. Journal of Reproductive Immunology. 2026;173:104805. doi:10.1016/j.jri.2025.104805.
[10] Bayrami A, Shirdel A, Rahim Pouran S, Mahmoudi F, Habibi-Yangjeh A, Singh R, Abdul Raman AA. Co-regulative effects of chitosan-fennel seed extract system on the hormonal and biochemical factors involved in the polycystic ovarian syndrome. Materials Science and Engineering: C. 2020;117:111351. doi:10.1016/j.msec.2020.111351.
[11] Heshmati J, Moini A, Sepidarkish M, Morvaridzadeh M, Salehi M, Palmowski A, Mojtahedi MF, Shidfar F. Effects of curcumin supplementation on blood glucose, insulin resistance and androgens in patients with polycystic ovary syndrome: A randomized double-blind placebo-controlled clinical trial. Phytomedicine. 2021;80:153395. doi:10.1016/j.phymed.2020.153395.
[12] Weng G, Li W, Qin F, Dong M, Yue S, Mehmood S, Wang X. Eco-friendly synthesis of zirconia nanoparticles using Sonchus asper extract: A sustainable approach to enhancing Chinese cabbage growth and remediating chromium-contaminated soil. Toxics. 2025;13(5):324. doi:10.3390/toxics13050324.
[13] Hosen ME, Rahman MA, Rahman MS, Akash S, Khalekuzzaman M, Alsahli AA, Bourhia M, Nafidi HA, Islam MA, Zaman R. Synthesis of Silver Nanoparticles Using Camellia sinensis Leaf Extract: Promising Particles for the Treatment of Cancer and Diabetes. Chemistry & Biodiversity. 2024;21(3). doi:10.1002/cbdv.202301661.
[14] Badawy A, Elnashar A. Treatment options for polycystic ovary syndrome. International Journal of Women's Health. 2011;3:25-35. doi:10.2147/IJWH.S11304.